DOI 10.1007/s11223-019-00115-3
Strength of Materials, Vol. 51, No. 4, July, 2019

EFFECT OF SAMPLING INTERVAL AND ANISOTROPY ON LASER SCANNING ACCURACY IN ROCK MATERIAL SURFACE ROUGHNESS MEASUREMENTS

S. M. Hu,[a,b] L. Huang,[c,1] Z. J. Chen,[a] Z. M. Ji,[a] and Z. Liu[d]

UDC 539.4

Three-dimensional laser scanning is an advanced technique for fracture roughness measurements. The surface roughness of fractures (discontinuities) accurately measured is of practical importance for proper evaluation of the mechanical properties of a fractured rock material. It is also appropriate to perform a more systematic study on the effect of a sampling interval on the roughness measurement accuracy. This effect was investigated based on the 3D-point-cloud data of a fracture surface acquired with laser scanning. A series of 2D profiles corresponding to twelve directions were extracted from concentric circular sampling windows of different diameters. The roughness measurement accuracy is quantified by the three parameters, viz the mean square first derivative Z_2, structure function SF, and roughness profile index R_p. The sampling interval effect was investigated for its different values by analyzing the three parameters of different profiles. It was established that SF was very sensitive, while Z_2 and R_p were less responsive to the sampling interval. It exerts a much weaker influence on the rock material fracture roughness in comparison with anisotropy.

Keywords: rock material fracture, rock discontinuity, surface roughness, sampling interval effect, three-dimensional laser scanning.

Introduction. The roughness of rock material fractures (called also discontinuities) plays an important role in the mechanical properties and behavior of the rock media [1–3]. Therefore, accurately measuring the fracture roughness becomes a fundamental problem in rock mechanics [4–8]. Roughness measurement techniques fall into two primary categories: (1) the contact techniques [9, 10] and (2) non-contact techniques [11, 12].

As an advanced non-contact technique, the three-dimensional laser scanning (3D-LS) is increasingly used to measure the rock material fracture roughness. Previous studies have shown that the sampling interval is important to the characterization of rock material fracture roughness in both 2D and 3D formulations [13–15]. Currently, in two-dimensional evaluation methods, most of the research on sampling interval effect has been focused on Barton's 10 typical profiles (a result of using a profile comb with a 1-mm distance between teeth) [15, 16], while there is very limited attention drawn to the sampling interval effect on 3D geometrical data of rock material fracture surface for the three-dimensional evaluation methods.

Therefore, the sampling interval effect of rock material fracture surface was analyzed in detail in this study, based on the 3D-point-cloud data acquired by the 3D-LS technique. Various concentric circular sampling windows

[a]School of Earth Sciences and Engineering, Hohai University, Nanjing, Jiangsu, China. [b]Jiangxi Engineering Research Center of Water Engineering Safety and Resources Efficient Utilization, Nanchang Institute of Technology, Nanchang, Jiangxi, China. [c]Three Gorges Research Center for Geohazards, Ministry of Education, China University of Geosciences, Wuhan, Hubei, China ([1]huanglei@cug.edu.cn, ORCID: 0000-0001-9991-0087). [d]Terracon Consultants, Inc., Greenville, SC, USA. Translated from Problemy Prochnosti, No. 4, pp. 201 – 211, July – August, 2019. Original article submitted October 20, 2018.

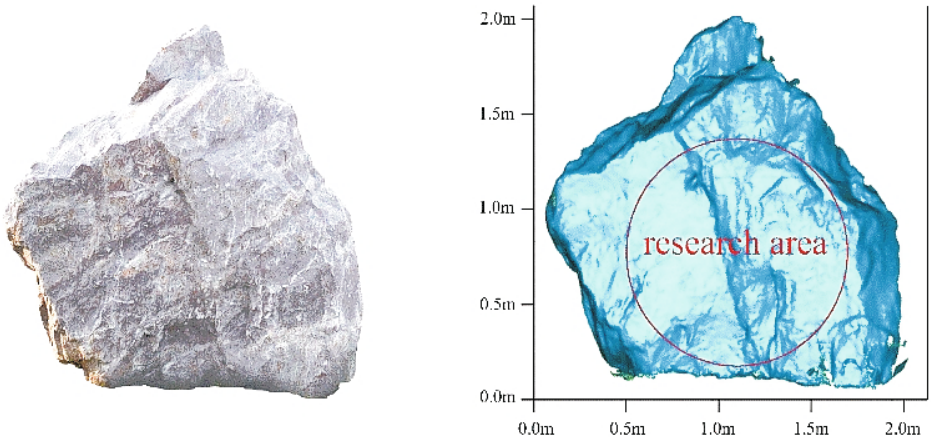

Fig. 1. Photo of a scanned sample (a) and the complete 3D surface roughness model acquired by 3D-LS (b). The research area is comprised in the circle with a diameter of 1.2 m.

with different diameters were acquired from the 3D surface roughness model, and a series of 2D profiles with different directions at angular increments of 15° were then extracted from each circular sampling window. Each profile was evaluated by three parameters: (1) the mean square first derivate Z_2, (2) the structure function SF, and (3) the roughness profile index R_p at different sampling intervals. These three parameters are widely used to evaluate the rock material fracture roughness and are respectively related to the roughness slope, the degree of change in roughness height, and the actual length of the profile.

1. Methodology of Investigation.

1.1. Specimen and Instrument. A granitic rock material specimen with an irregular size of approximately 4 m^3, was considered for the investigation, and a sampling window circle with a diameter of 1.2 m on the specimen was extracted (Fig. 1). The specimen was collected from the Geological Science and Technology Park, which belongs to the National and Provincial Joint Engineering Laboratory for the Hydraulic Engineering Safety and Efficient Utilization of Water Resources of Poyang Lake Basin, China. The sample can be described as a massive blocky, slightly weathered, light red medium-grained granite, with striations on the surface.

A 3D terrestrial scanner Riegl VZ-1000 from the National and Provincial Joint Engineering Laboratory for the Hydraulic Engineering Safety and Efficient Utilization of Water Resources of Poyang Lake Basin, was mounted on a tripod 1.2 m above the ground and approximately 5.0 m directly in front of the rock face to digitize a rock specimen with the resolution of 0.04°.

1.2. Investigation Procedure. The purpose of this investigation is to (1) clarify the possible sampling interval effect on the measurement accuracy of roughness, and (2) test this effect against the anisotropy effect. The investigation follows a four-step process: Step I – scanning and processing of the 3D point clouds; Step II – extraction of 2D-linear profiles; Step III – extraction of discrete points; and Step IV – evaluation of the rock material fracture roughness.

Step 1. Scanning and Processing of 3D Point Clouds Data. After recording the rock material specimen in the form of point clouds data by 3D-LS technique, the 3D Point clouds data process consists of 4 steps: (1) removing useless point cloud data to focus on the region of interest, as for a 360° panorama was acquired by 3D-LS; (2) reducing the noise in the raw point clouds of the region of interest (ROI); (3) reconstructing the rock surface from the de-noised point clouds data by the Geomagic software; (4) coordinate transformation, including plane fitting and rotation.

Step 2. Extraction of 2D-Linear Profiles. Various concentric circular sampling windows were extracted with a diameter of 2, 4, 6, 8, 10, 12, 14, 16, 18, 20, 30, 40, 50, 60, 70, 80, 90, 100, 110, and 120 cm, respectively, and a series of 2D profiles with the directions of 0, 15, 30, 45, 60, 75, 90, 105, 120, 135, 150, and 165°, respectively, were

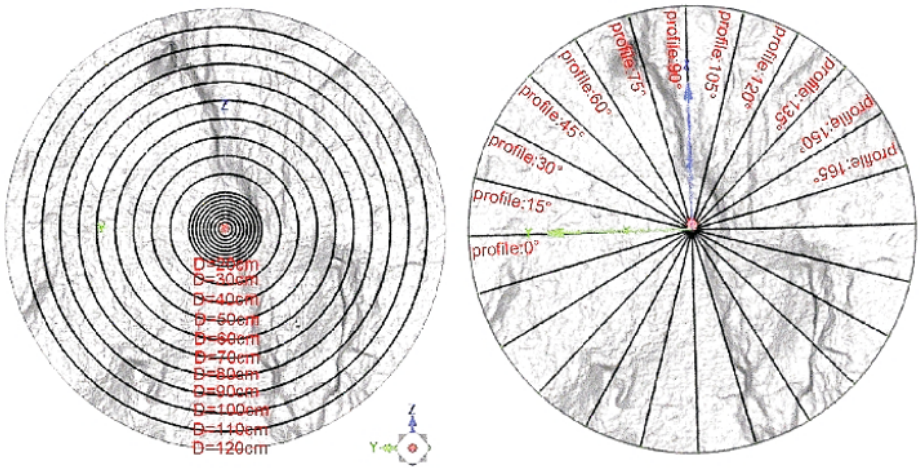

a b

Fig. 2. (a) A series of concentric circular sampling windows were extracted with a diameter of 2, 4, 6, 8, 10, 12, 14, 16, 18, 20, 30, 40, 50, 60, 70, 80, 90, 100, 110, and 120 cm, respectively; (b) example of twelve 2D profiles extracted from a square sampling window ($D = 1.2$ m).

then extracted from each circular sampling window. Figure 2 presents the extraction of the sampling windows and 2D profiles. The 2D profiles were finally converted into lines in two-dimensional coordinate system after their alignment.

Step 3. *Extraction of Discrete Points*. For the evaluation of rock fracture roughness, constructed curves should be converted into discrete points. The detailed steps are listed as follows: (1) profiles were extracted through the Geomagic software, and changed into dxf format files; (2) profiles in dxf format were changed into discrete points in txt format files by auto-lisp function. Thus, Z_2, SF, and R_p values can be calculated via the MATLAB software.

Step 4. *Evaluation of the Rock Material Fracture Roughness.* Various statistical parameters were used to evaluate the rock material fracture roughness in the previous research. It was found that Z_2, SF, and R_p are related to the roughness slope, degree of change in roughness height, and the profile actual length, respectively. In this study, Z_2, SF, and R_p were used as the evaluation indices of the joint roughness coefficient (JRC) to analyze the sampling interval effect. For every circular sampling window, Z_2, SF, and R_p values in different directions ranging from 0 to 165° at angular increments of 15° were calculated with sampling intervals of 0.2, 0.4, 0.8, 1.6, and 3.2 mm, respectively. Values of Z_2, SF, and R_p were determined using the following equations:

$$Z_2 = \left[\frac{1}{L}\int_{x=0}^{x=L}\left(\frac{dy}{dx}\right)^2\right]^{1/2} = \left[\frac{1}{L}\sum_{i=1}^{n-1}\frac{y_{i+1}-y_i}{x_{i+1}-x_i}\right]^{1/2}, \tag{1}$$

$$SF = \frac{1}{L}\int_{x=0}^{x=L}[f(x+dx)-f(x)]^2\,dx = \frac{1}{L}\sum_{i=1}^{n-1}(y_{i+1}-y_i)^2(x_{i+1}-x_i), \tag{2}$$

$$R_p = \frac{\sum_{i=1}^{n-1}[(x_{i+1}-x_i)^2+(y_{i+1}-y_i)^2]^{1/2}}{L}, \tag{3}$$

where y_i is the height of a rock material fracture profile at x_i, dx is the sampling interval between x_i and x_{i+1}, and L is the normalized length of the rock material fracture profile.

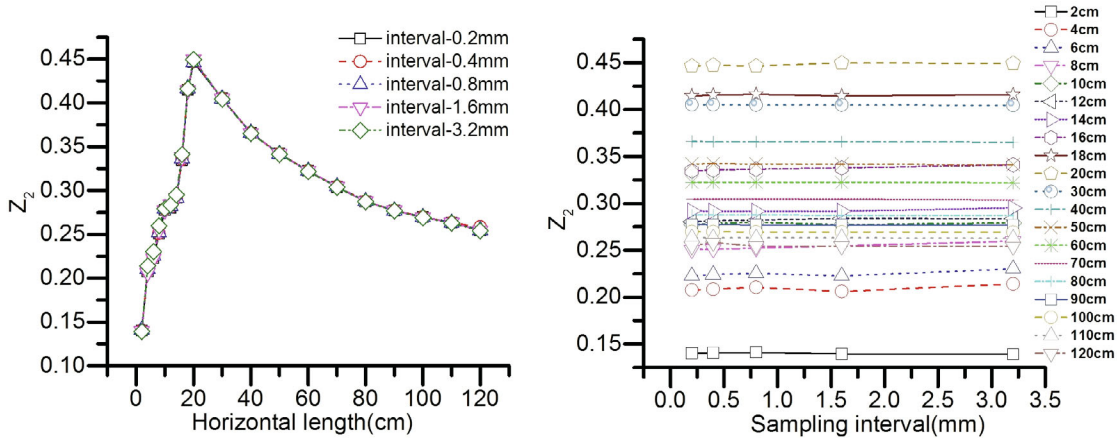

a b

Fig. 3. (a) Variation of Z_2 with the sampling interval in profile 0°; (b) variation of Z_2 with L in profile 0°.

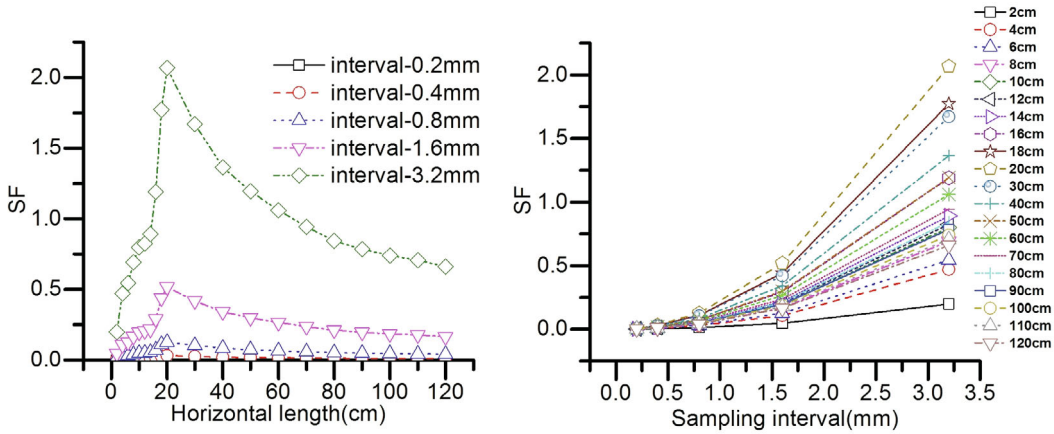

a b

Fig. 4. (a) Variation of SF with the sampling interval in profile 0°; (b) variation of SF with L in profile 0°.

2. Results.

2.1. Sampling Interval Effect. For the profile in the direction of 0°, Z_2 almost does not vary with sampling intervals as $L = [2\text{ cm}, 120\text{ cm}]$ (Fig. 3a); SF is sensitive to the sampling interval, and SF increases exponentially as the sampling interval increases (Fig. 4a); R_p varies significantly as $L \le 20$ cm (Fig. 5a), while R_p varies very little with sampling interval as $L > 20$ cm (Fig. 5b). As for the effect of L on parameters Z_2, SF, and R_p, the overall tendency is that at $L \le 20$ cm, values of Z_2, SF, and R_p increase sharply as L increases; Z_2, SF, and R_p are approximately maximal at $L = 20$ cm; the values of Z_2, SF, and R_p decrease sharply at 20 cm $< L <$ 80 cm, and remain unchanged at $L \ge 80$ cm (Figs. 3b, 4b, and 5c).

For the profile in the direction of 90°, Z_2 varies very little with sampling interval at the normalized length 2 cm $< L <$ 120 cm (Fig. 6a); SF is sensitive to the sampling interval, and the overall tendency of SF is that it increases exponentially as the sampling interval increases (Fig. 7a); R_p varies for $L \le 40$ cm (Fig. 8a), in contrast to small variation for $L > 40$ cm (Fig. 8b). As for the influence of L on parameters Z_2, SF, and R_p, the overall tendency is that at $L \le 40$ cm, Z_2 and SF increase sharply with L and is consistent at $L > 40$ cm (Figs. 6b and 7b). R_p is scattered at $L \le 40$ cm (especially at $L \le 20$ cm) and trends to be consistent at $L > 40$ cm (Fig. 8c).

2.2. Comparison with the Anisotropy Effect. Furthermore, to examine the sampling interval effect of the 2D roughness parameters Z_2, SF, and R_p in comparison to the anisotropy effect, a series of twelve 2D profiles at $L = 120$ cm (for 0, 15, 30, 45, 60, 75, 90, 105, 120, 135, 150, and 165°, respectively) were extracted at angular

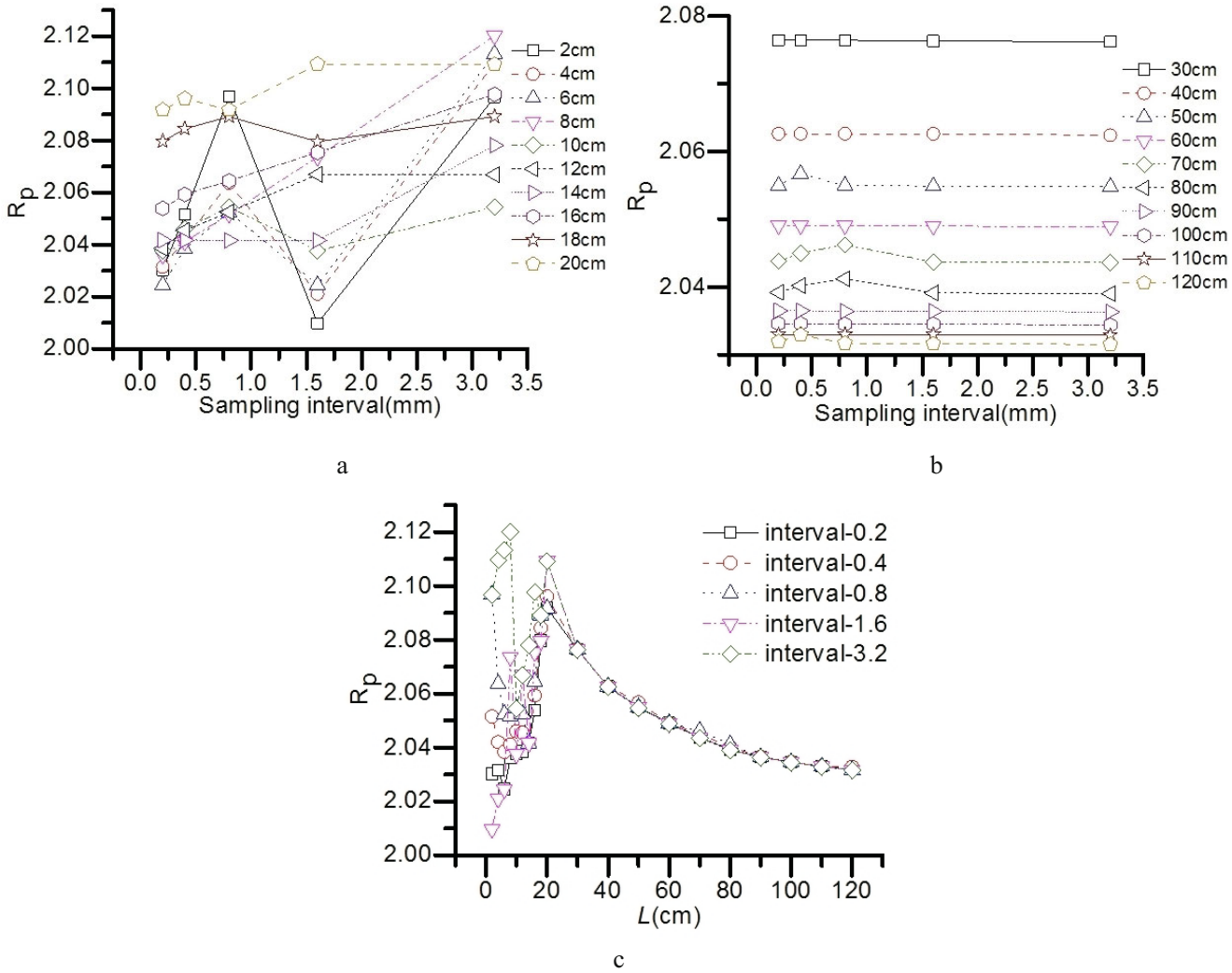

Fig. 5. (a) Variation of R_p with the sampling interval as $L \leq 20$ cm in profile 0°; (b) variation of R_p with the sampling interval as $L > 20$ cm in profile 0°; (c) variation of R_p with L in profile 0°.

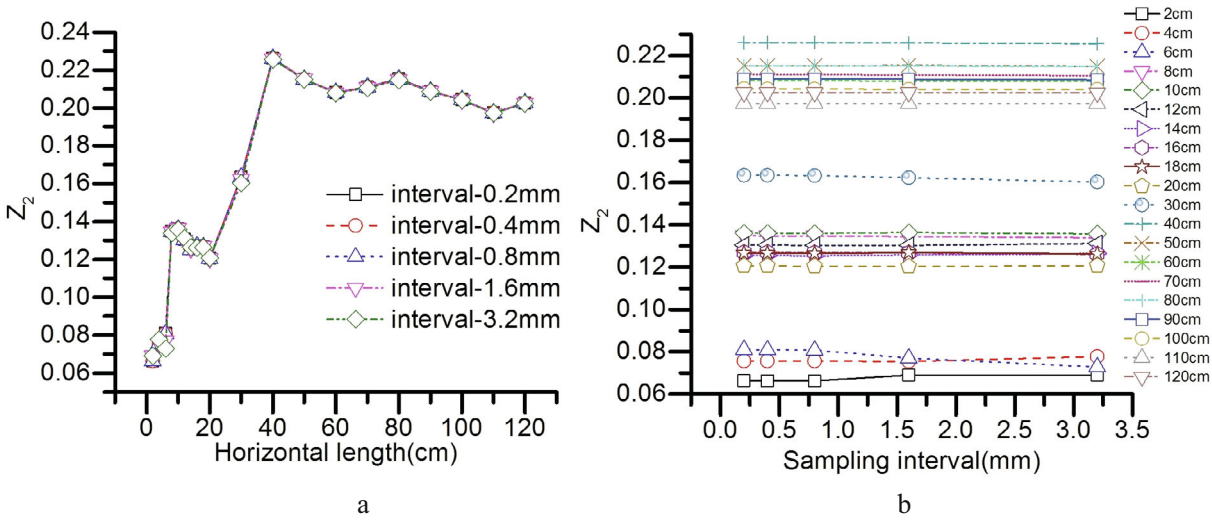

Fig. 6. (a) Variation of Z_2 with the sampling interval in profile 90°; (b) variation of Z_2 with L in profile 90°.

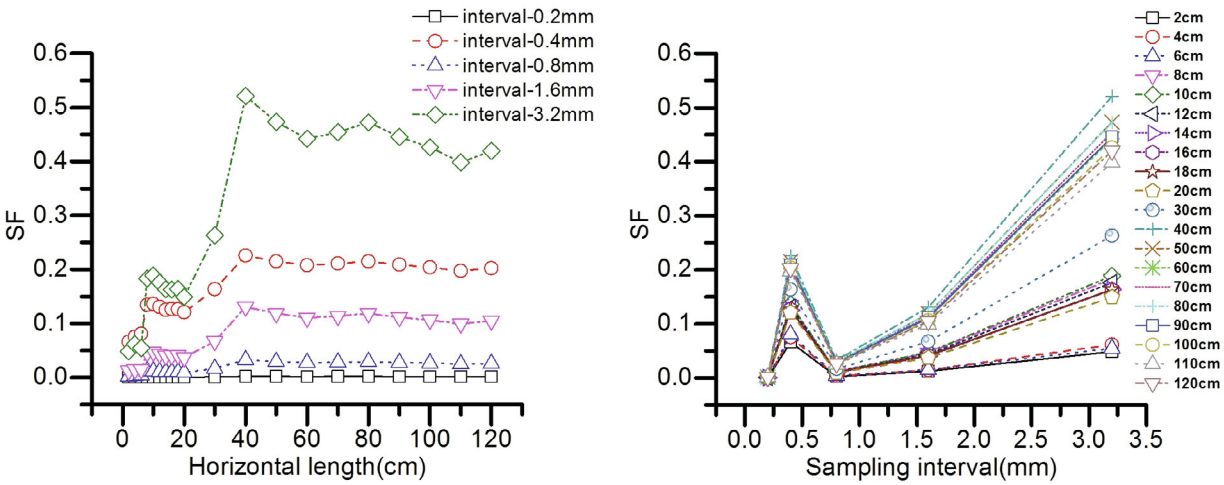

a b

Fig. 7. (a) Variation of SF with the sampling interval in profile 90°; (b) variation of SF with L in profile 90°.

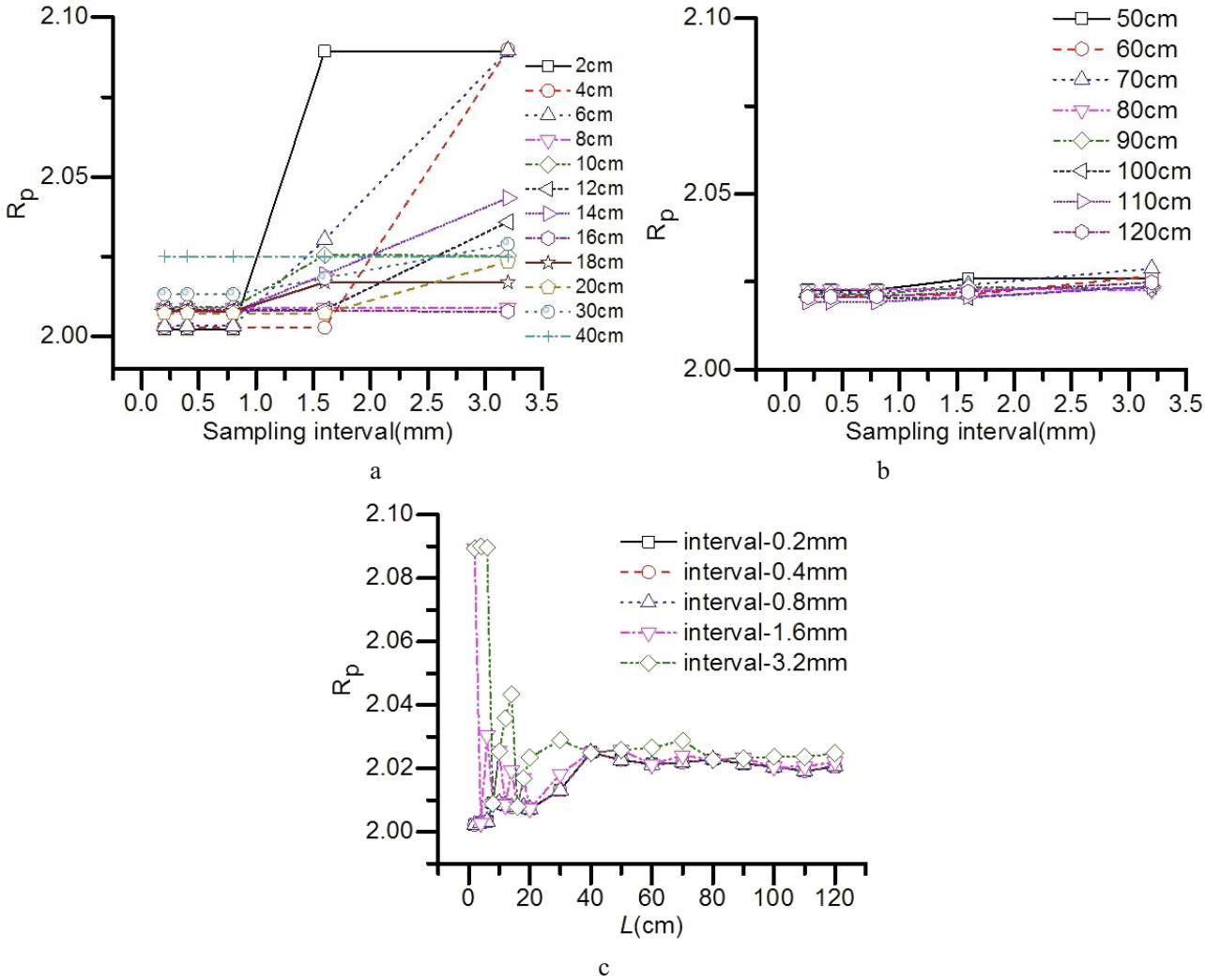

a b c

Fig. 8. (a) Variation of R_p with the sampling interval as $L \le 40$ cm in profile of 90°; (b) variation of R_p with the sampling interval at $L > 40$ cm in profile of 90°; (c) variation of R_p with L in profile of 90°.

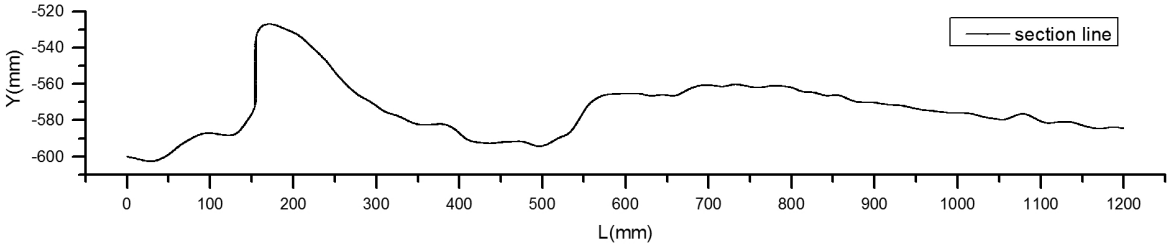

Fig. 9. The profile in 45° direction.

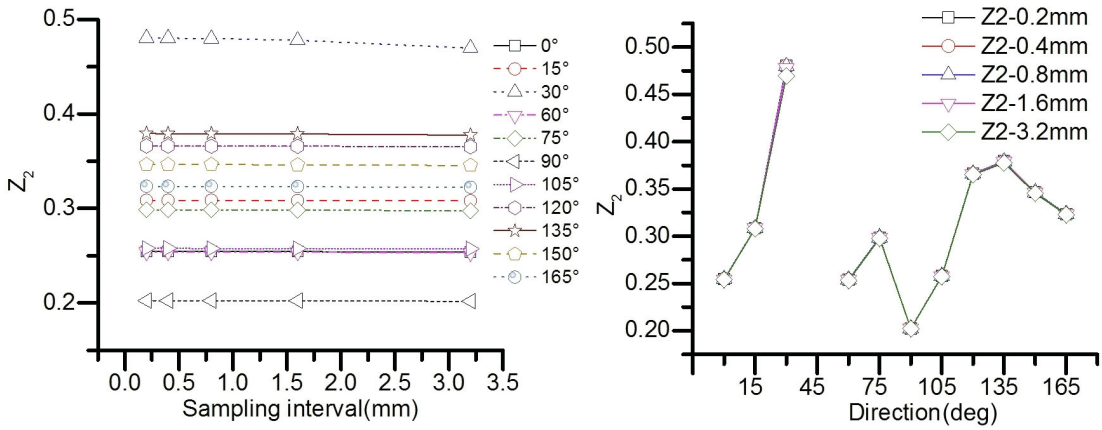

a b

Fig. 10. (a) Variation of Z_2 with the sampling interval between different directions; (b) variation of Z_2 with the directions between different sampling intervals.

increments of 15° and analyzed. However, the profile at the direction of 45° was almost vertical at $L = [153.5$ cm, 153.9 cm] (Fig. 9), and results in the Z_2 value be infinite, and SF and R_p values were much larger than those in other directions. The reason is that the 3D point clouds collected by 3D-LS are much more precise, as compared to the traditional methods such as the Barton comb [17], contour gauge [18], and profile gauge [19]. With the expansion of digital technologies, this profile extraction method will be widely used, and the extreme phenomenon will still be hard to avoid in the future. The suggested solution is to use microtranslation when extracting profiles or local adjustment of the extracted profiles.

In this study, Z_2 varies very slightly with sampling intervals in any direction, except for that of 45°, which trends to be infinite (Fig. 10a), while Z_2 varies between different directions (Fig. 10b). SF increases with sampling intervals in any direction, and SF is sensitive to the sampling interval (Fig. 11a), while SF differs for various directions (Fig. 11b). At the direction of 45°, SF is different from the value in other directions, and it tends to be consistent with them if the sampling interval exceeds 1.6 mm (Fig. 11b). R_p almost does not vary with sampling intervals in any direction, except for of 45° (Fig. 12a), and R_p is almost the same for any direction (Fig. 12b). At 45°, R_p is different from its values in other directions and tends to be consistent when the sampling interval is no less than 1.6 mm (Fig. 12a).

In order to quantify the sampling interval and anisotropy effects, the relative deviation factor (F) was introduced in the following form:

$$F = \frac{\max(X) - \min(X)}{\text{average}(X)}, \tag{4}$$

where X refers to Z_2, SF, and R_p.

The relative deviation factor of sampling interval effect means that F is calculated if the direction is certain (Table 1), while the relative deviation factor of anisotropy effect indicates that F was calculated for a certain

TABLE 1. Results on the Relative Deviation Factor for the Sampling Interval Effect

Direction	F			Direction	F		
(deg)	Z_2	SF	R_p	(deg)	Z_2	SF	R_p
0	0.002	3.736	0.000	90	0.003	3.736	0.000
15	0.002	3.736	0.000	105	0.002	3.736	0.000
30	0.022	3.704	0.000	120	0.002	3.736	0.000
45	N/A	1.441	0.457	135	0.004	3.733	0.000
60	0.004	3.734	0	150	0.003	3.734	0.000
75	0.004	3.732	0	165	0.002	3.735	0.000

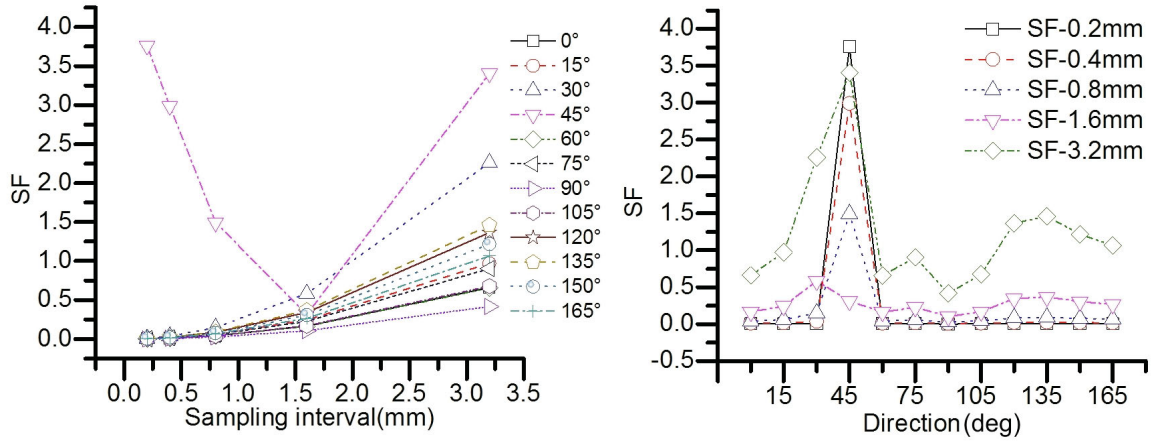

a b

Fig. 11. (a) Variation of SF with the sampling interval between different directions; (b) variation of SF with the directions between different sampling intervals.

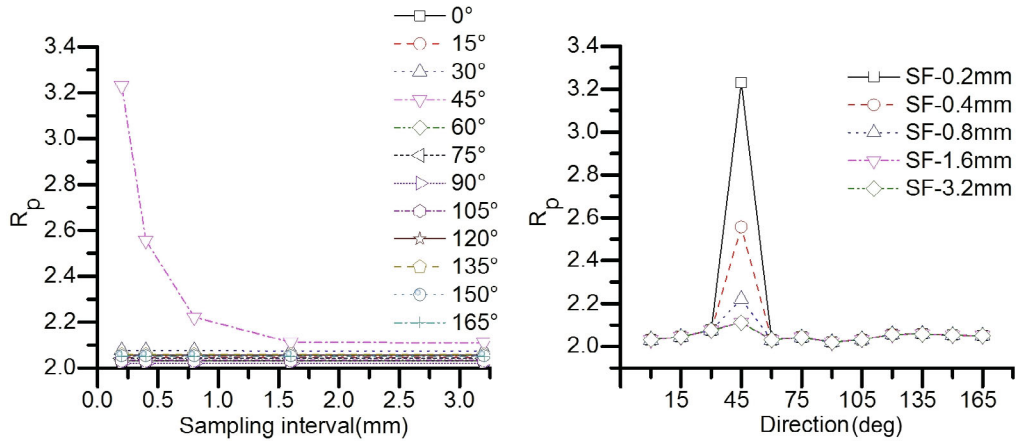

a b

Fig. 12. (a) Variation of R_p with the sampling interval between different directions; (b) variation of R_p with the directions between different sampling intervals.

sampling interval (Table 2). The relative deviation factor of anisotropy effect is much larger than the sampling interval effect.

By comparing the relative deviation factors of sampling interval and anisotropy, it is seen that the sampling interval has a much weaker influence on the rock material fracture roughness than anisotropy.

TABLE 2. Results of the Relative Deviation Factor for the Anisotropy Effect

Sampling interval (mm)	F				
	Z_2	SF	SF*	R_p	R_p*
0.2	0.880	1.808	11.849	0.027	0.009
0.4	0.880	1.807	11.277	0.027	0.009
0.8	0.878	1.803	7.890	0.027	0.009
1.6	0.874	1.793	0.768	0.027	0.009
3.2	0.853	1.793	2.380	0.027	0.009

* Calculated for the direction of 45°.

3. Discussion and Implications. Most of the traditional methods to measure the surface roughness of rock material fractures are two-dimensional contact methods, and L is often limited within 10–20 cm. However, as indicated in this study, L should be long enough (the effective value of the case in this study is 80 cm). Thus the values of Z_2, SF, and R_p can accurately reflect the overall roughness of the rock surface. The 3D-LS technique is a non-contact, three-dimensional method, which overcomes the size limitation of measurement during field investigation and provides a higher efficiency and accuracy than traditional methods in characterizing the structure surface.

The main finding of this study is that the difference in Z_2 and R_p values obtained for different sampling intervals is very small, while SF is very sensitive to the sampling interval. The JRC values are found to be more accurate when calculated via Z_2 and R_p, instead of SF, especially when the 3D point cloud data are not dense enough. This complies with results of other researchers. Thus, Ge et al. [15] reported that the amplitude of the variation in the range intervals of 10~110 cm was less than that in the range of 110~1000 cm, and 110 cm could be considered an effective sampling interval. However, sampling intervals in some cases range from 10 to 1000 cm. Therefore, this conclusion is applicable to characterizing large-scale fracture in situ but not under laboratory test conditions. Based on Barton's 10 typical profiles, with a JRC value ranging from 0.4 to 18.7, Jang et al. [14] implied that Z_2 and R_p values dropped with the sampling interval. However, for specific conditions or rock material fracture surfaces, the variation of JRC value will be much smaller; as a result, Z_2 and R_p values for different sampling intervals will be consistent. The variation of SF revealed in the present study complies with findings in [14].

Conclusions. Based on the observations and analysis presented in this paper, the major conclusions regarding the sampling interval effect of rock material fracture are as follows:

1. The measurement of rock material fracture surface roughness by 3D-LS can provide a higher efficiency and accuracy in characterizing the rock material fracture surface.

2. SF is very sensitive to the sampling interval, and Z_2 and R_p are consistent between different sampling intervals for a specific project or rock material fracture surfaces.

3. It is noted that the sampling interval has a much weaker influence on the rock material fracture roughness than the anisotropy. It is vital to have a good observation for the shear direction of the rock material fracture in engineering practice.

Acknowledgments. This research was supported by four funds, namely the Science and Technology Project of Jiangxi Provincial Transportation Department (No. 2017H0018), the Open Foundation of Jiangxi Engineering Research Center of Water Engineering Safety and Resources Efficient Utilization (No. OF201602; No. OF201604), and Zhejiang Collaborative Innovation Center for Prevention and Control of Mountain Geological Hazards (No. PCMGH-2017-Z03). The authors would also like to thank Chenghui Wan, and Zongjun Wu for their assistance.

REFERENCES

1. L. Huang, H. Tang, Q. Tan, et al., "A novel method for correcting scanline-observational bias of discontinuity orientation," *Sci. Rep*., **6**, 22942 (2016).

2. H. M. Tang, L. Huang, A. Bobet, et al., "Identification and mitigation of error in the Terzaghi bias correction for inhomogeneous material discontinuities," *Strength Mater.*, **48**, No. 6, 825–833 (2016).
3. H. Tang, L. Huang, C. H. Juang, and J. Zhang, "Optimizing the Terzaghi estimator of the 3D distribution of rock fracture orientations," *Rock Mech. Rock Eng.*, **50**, No. 8, 2085–2099 (2017).
4. N. Fardin, O. Stephansson, and L. Jing, "The scale dependence of rock joint surface roughness," *Int. J. Rock Mech. Min. Sci.*, **38**, No. 5, 659–669 (2001).
5. D. H. Kim, I. Gratchev, and A. Balasubramaniam, "Determination of joint roughness coefficient (JRC) for slope stability analysis: a case study from the Gold Coast area, Australia," *Landslides*, **10**, No. 5, 657–664 (2013).
6. G. Zhang, M. Karakus, H. Tang, et al., "A new method estimating the 2D joint roughness coefficient for discontinuity surfaces in rock masses," *Int. J. Rock Mech. Min. Sci.*, **72**, 191–198 (2014).
7. P. Alameda-Hernández, J. Jiménez-Perálvarez, J. A. Palenzuela, et al., "Improvement of the JRC calculation using different parameters obtained through a new survey method applied to rock discontinuities," *Rock Mech. Rock Eng.*, **47**, No. 6, 2047–2060 (2014).
8. X. Wang, L. Huang, C. Yan, and B. Lian, "HKCV rheological constitutive model of mudstone under dry and saturated conditions," *Adv. Civil Eng.*, **2018**, 2621658 (2018), https://doi.org/10.1155/2018/2621658.
9. X. Li, J. Chen, and H. Zhu, "A new method for automated discontinuity trace mapping on rock mass 3D surface model," *Comput. Geosci.*, **89**, 118–131 (2016).
10. A. J. Riquelme, R. Tomás, and A. Abellán, "Characterization of rock slopes through slope mass rating using 3D point clouds," *Int. J. Rock Mech. Min. Sci.*, **84**, 165–176 (2016).
11. B. S. Tatone and G. Grasselli, "An investigation of discontinuity roughness scale dependency using high-resolution surface measurements," *Rock Mech. Rock Eng*., **46**, No. 4, 657–681 (2013).
12. J. Chen, H. Zhu, and X. Li, "Automatic extraction of discontinuity orientation from rock mass surface 3D point cloud," *Comput. Geosci.*, **95**, 18–31 (2016).
13. Z. C. Tang, Y. Y. Jiao, L. N. Y. Wong, and X. C. Wang, "Choosing appropriate parameters for developing empirical shear strength criterion of rock joint: review and new insights," *Rock Mech. Rock Eng.*, **49**, No. 11, 4479–4490 (2016).
14. H. S. Jang, S. S. Kang, and B. A. Jang, "Determination of joint roughness coefficients using roughness parameters," *Rock Mech. Rock Eng.*, **47**, No. 6, 2061–2073 (2014).
15. Y. Ge, H. Tang, M. M. E. Eldin, et al., "A description for rock joint roughness based on terrestrial laser scanner and image analysis," *Sci. Rep.*, **5**, 16999 (2015).
16. Z. Y. Yang, S. C. Lo, and C. C. Di, "Reassessing the joint roughness coefficient (JRC) estimation using Z_2," *Rock Mech. Rock Eng.*, **34**, No. 3, 243–251 (2001).
17. N. Barton and V. Choubey, "The shear strength of rock joints in theory and practice," *Rock Mech*., **10**, Nos. 1–2, 1–54 (1977).
18. G. Weissbach, "A new method for the determination of the roughness of rock joints in the laboratory," *Int. J. Rock Mech. Min. Sci. Geomech. Abstr.*, **15**, No. 3, 131–133 (1978).
19. B. Stimpson, "A rapid field method for recording joint roughness profiles," *Int. J. Rock Mech. Min. Sci. Geomech. Abstr.*, **19**, No. 6, 345–346 (1982).